Validating Two Novel Equivalent Impedance Estimators

Paul Cuffe, *Member, IEEE,* and Federico Milano *Fellow, IEEE*

***Abstract*—Various local voltage stability indices use an equivalent impedance to characterise the wider power system. This letter proposes two new ways of inferring an appropriate equivalent impedance from a power system's admittance matrix. Continuation power flow simulations are used to validate the quality of the new estimators, and to benchmark them against some earlier approaches.**

I. Introduction

Circuit theory shows that the maximum power deliverable to a load will occur when its impedance matches the feeding Thévenin impedance, and this concept underpins various approaches to appraising a bus' voltage stability [1]–[3] Such indices typically infer an equivalent impedance using sequential samples of local voltage and current [4]. A recent review [5] noted one shortcoming of such approaches: *"these indices are very sensitive to the small change of the data"* and went on to suggest that future work in voltage stability should propose a measure that *"considers the Thévenin network impedance and is insensitive to the small change of the two consecutive measurement data"* Accordingly, the present letter proposes and compares two new ways to directly infer an equivalent impedance from a system's admittance matrix. While an equivalent impedance alone cannot capture all aspects of voltage stability (due to e.g. machine reactive power limits) their more accurate estimation can offer insights on how network structure affects bus loadability.

II. Methodology

Alongside the two novel approaches, two established techniques are also used to populate the vector of network equivalent impedance estimators as seen by each load, $\boldsymbol{z}_L$.

A. Proposed new estimators

1) Load submatrix impedance: The $\boldsymbol{Y}_{\text{bus}}$ is reordered, per [1], such that the m generator buses and n load buses are grouped together:

$$\begin{bmatrix}\boldsymbol{i}_G\\ \boldsymbol{i}_L\end{bmatrix} = \begin{bmatrix}\boldsymbol{Y}_{GG} & \boldsymbol{Y}_{GL}\\ \boldsymbol{Y}_{LG} & \boldsymbol{Y}_{LL}\end{bmatrix}\begin{bmatrix}\boldsymbol{v}_G\\ \boldsymbol{v}_L\end{bmatrix} \tag{1}$$

Manipulation of (1) gives:

$$\boldsymbol{v}_L = \boldsymbol{Z}_{LL}\boldsymbol{i}_L + \boldsymbol{F}_{LG}\boldsymbol{v}_G \tag{2}$$

Where $\boldsymbol{Z}_{LL} = \boldsymbol{Y}_{LL}^{-1}$ and $\boldsymbol{F}_{LG} = -\boldsymbol{Z}_{LL}\boldsymbol{Y}_{LG}$. Recent work [6] has shown that the rows of $\boldsymbol{F}_{LG}$ sum close to one with negligible imaginary components: it thus shows the different participation each generator has in establishing the no-load voltage at a particular bus. Therefore, the diagonal elements of $\boldsymbol{Z}_{LL}$ have a clear interpretation as system effective impedances at each bus, as they explicitly describes the voltage drop caused by local current consumption (see [7] for more on this paradigm) Therefore, an impedance estimate is given by:

$$\boldsymbol{z}_L^{\text{Sub}} = \text{diag}(\boldsymbol{Z}_{LL}) \tag{3}$$

2) Klein resistance distance: The $\boldsymbol{Z}_{\text{bus}}$ matrix (elements z_{ij}) is the inverse of the $\boldsymbol{Y}_{\text{bus}}$ matrix. According to Klein [8], the Thévenin impedance between buses i and j is calculated using these elements of the $\boldsymbol{Z}_{\text{bus}}$ matrix:

$$z_{ij}^{\text{k}} = z_{ii} + z_{jj} - z_{ij} - z_{ji} \tag{4}$$

Various works have used the intuition that the electrically-nearest generator to a load represents information relevant to creating a Thévenin equivalent [9], [10]. While those works used approximations, the full $\boldsymbol{Z}^{\text{k}}$ matrix of internode impedances allows the extraction of the explicit Thévenin distance between each load and its nearest generator:

$$\boldsymbol{z}_L^{\text{Near}} = \min_{j\in L} z_{ij}^k, \qquad i = 1, ..., m \tag{5}$$

B. Comparative estimators

1) Shortest path impedance: Work in [9] used network traversal techniques to find the shortest topological path between each load and its nearest generator. The sum of branch impedances along this geodesic path was used in [9] as an estimate of the system equivalent impedance: $\boldsymbol{z}_L^{\text{Topo}}$.

2) Driving point impedance: The main diagonal of the $\boldsymbol{Z}_{\text{bus}}$ matrix contains *driving point impedances* which describe the short circuit power available at a bus. Some authors have likened these with a Thévenin equivalent of the system, at least under faulted conditions [11].

$$\boldsymbol{z}_L^{\text{Driving}} = \text{diag}(\boldsymbol{Z}_{\text{bus}}) \tag{6}$$

C. Estimator quality assessment

Each estimators is used to predict the maximum loadability at each bus. For a unity power factor, the forecasted maximum active power is given as function of $\boldsymbol{z}_L(=\boldsymbol{r}_L + j\boldsymbol{x}_L)$ by [12]:

$$\boldsymbol{p}^+ = \frac{\boldsymbol{v}_L^2}{2(\sqrt{\boldsymbol{r}_L^2 + \boldsymbol{x}_L^2} + \boldsymbol{r}_L)} \tag{7}$$

The empirical steady state loading limits at each bus are calculated using continuation power flow techniques [13], where each load is *individually* increased. The extra load is served from local generators as identified in the $\boldsymbol{F}_{LG}$ matrix, without regard to machine active or reactive power limits (this

P. Cuffe and F. Milano are with the School of Electrical and Electronic Engineering, University College Dublin.

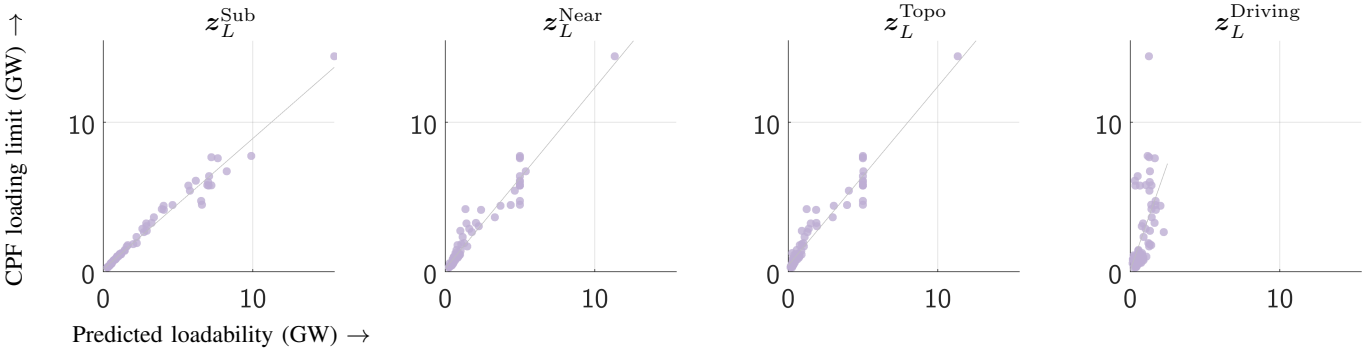

Fig. 1. Scatterplots showing the predictive efficacy of each estimator for maximum active power loadability in the `nesta_case118_ieee` system

TABLE I.
MAPE OF LOADABILITY FORECASTS $\boldsymbol{p}^+$ BASED ON EACH $\boldsymbol{z}_L$

	z_L^{Sub}	z_L^{Near}	z_L^{Topo}	z_L^{Driving}
nesta_case30_ieee	16	26	46	89
nesta_case39_epri	27	35	38	74
nesta_case57_ieee	12	14	40	80
nesta_case73_ieee_rts	14	28	37	52
nesta_case89_pegase	20	52	53	100
nesta_case118_ieee	7.7	25	39	47
nesta_case162_ieee_dtc	46	24	41	187
nesta_case189_edin	40	43	41	69
nesta_case300_ieee	24	28	38	49

simplified procedure identifies just saddle-node, rather than limit-induced, bifurcations)

Comparisons between the predicted and empirical maximum loadings can then be used to gauge the quality of the different $\boldsymbol{z}_L$ estimators.

III. Results & Conclusions

The estimators and loadabilities were calculated in [13] using nine medium sized test systems from [14]. In each case, $\boldsymbol{v}_L$ was set $= 1$ for consistency, although the $\boldsymbol{F}_{LG}$ matrix could perhaps be used to calculate a more accurate Thévenin voltage estimate. The quality of the $\boldsymbol{p}^+$ predictions for each estimator, on each system, are shown in Table I, which uses conditional formatting to show the *Mean Average Percentage Error* (MAPE) of these forecasts. The $\boldsymbol{z}_L^{\text{Sub}}$ estimator exhibits the best performance, again showing the insights that the $\boldsymbol{Z}_{LL}$ matrix can offer. The Klein resistance distance approach also shows some promise, with the $\boldsymbol{z}_L^{\text{Near}}$ estimator outperforming $\boldsymbol{z}_L^{\text{Topo}}$, as the latter doesn't consider the inherently paralell nature of impedances with a meshed transmission system. Finally, Table I shows that $\boldsymbol{z}_L^{\text{Driving}}$ is wholly unsuited to predicting saddle-node loadability limits.

Another view of the data is given in Fig. 1, which shows predicted versus empiric loadabilities for each estimator on the `nesta_case118_ieee` system. The clear linear trend for the $\boldsymbol{z}_L^{\text{Sub}}$ estimator is apparent, with most datapoints clustered tightly around the regression line.

References

[1] P. Kessel and H. Glavitsch, "Estimating the voltage stability of a power system," *IEEE Transactions on Power Delivery*, vol. 1, no. 3, pp. 346–354, 1986.

[2] I. Smon, G. Verbic, and F. Gubina, "Local voltage-stability index using Tellegen's theorem," *IEEE Transactions on Power Systems*, vol. 21, no. 3, pp. 1267–1275, 2006.

[3] A. Wiszniewski, "New criteria of voltage stability margin for the purpose of load shedding," *IEEE Transactions on Power Delivery*, vol. 22, no. 3, pp. 1367–1371, Jul. 2007.

[4] K. Vu, M. M. Begovic, D. Novosel, and M. M. Saha, "Use of local measurements to estimate voltage-stability margin," *IEEE Transactions on Power Systems*, vol. 14, no. 3, pp. 1029–1035, 1999.

[5] J. Modarresi, E. Gholipour, and A. Khodabakhshian, "A comprehensive review of the voltage stability indices," *Renewable and Sustainable Energy Reviews*, vol. 63, pp. 1–12, 2016.

[6] I. K. Dassios, P. Cuffe, and A. Keane, "Visualizing voltage relationships using the unity row summation and real valued properties of the F_{LG} matrix," *Electric Power Systems Research*, vol. 140, pp. 611–618, 2016.

[7] S. M. Abdelkader, D. J. Morrow, and A. J. Conejo, "Network usage determination using a transformer analogy," *IET Generation, Transmission Distribution*, vol. 8, no. 1, pp. 81–90, Jan. 2014.

[8] D. J. Klein and M. Randić, "Resistance distance," *Journal of mathematical chemistry*, vol. 12, no. 1, pp. 81–95, 1993.

[9] B. Genêt and J.-C. Maun, "Voltage-stability monitoring using wide-area measurement systems," in *Power Tech, 2007 IEEE Lausanne*, IEEE, 2007, pp. 1712–1717.

[10] S. Pérez-Londoño, L. Rodrzíguez, and G. Olivar, "A simplified voltage stability index SVSI," *International Journal of Electrical Power & Energy Systems*, vol. 63, pp. 806–813, 2014.

[11] N. D. Tleis, *Power systems modelling and fault analysis: theory and practice*. Elsevier, 2008.

[12] T. Cutsem, *Voltage stability of electric power systems*. New York: Springer, 2008, ISBN: 978-0-387-75536-6.

[13] R. D. Zimmerman, C. E. Murillo-Sánchez, and R. J. Thomas, "Matpower: steady-state operations, planning, and analysis tools for power systems research and education," *IEEE Transactions on power systems*, vol. 26, no. 1, pp. 12–19, 2011.

[14] C. Coffrin, D. Gordon, and P. Scott, "NESTA, the NICTA energy system test case archive," *arXiv preprint arXiv:1411.0359*, 2014.